Eur. J. Mineral.
2002, **14**, 905–914

Serpentinites from Central Cuba: petrology and HRTEM study

ANNE-LINE AUZENDE[1*], BERTRAND DEVOUARD[1], STÉPHANE GUILLOT[2], ISABELLE DANIEL[2], ALAIN BARONNET[3] and JEAN-MARC LARDEAUX[2]

[1] Laboratoire „Magmas et volcans“, UBP-CNRS-OPGC, 5 rue Kessler, F-63038 Clermont-Ferrand cedex, France
* Contact information, e-mail: auzende@opgc.univ-bpclermont.fr
[2] Laboratoire „Dynamique de la lithosphère“, CNRS-UCBL-ENSL, 11 boulevard du 11 novembre, F-69622 Villeurbanne cedex, France
[3] Centre de Recherche sur les Mécanismes de la Croissance Cristalline, CNRS, campus de Luminy, F-13288 Marseille cedex 09, France

Abstract: We have sampled serpentinites and the closely associated metabasites in the paleosubduction zone context of Central Cuba in order to characterise the microstructures of serpentine minerals as a function of metamorphic grade. The samples were collected in the eclogitic unit of the Escambray Massif and in the Zaza Zone, where eclogitic conditions were locally attained. Serpentinites are associated to the metabasites in lenses embedded in a metasediment matrix (Escambray) or form the matrix that embeds the metabasites (Zaza Zone). Field and petrological evidence suggests that serpentinites and associated metabasites underwent the same metamorphic history. Serpentinites from the Escambray Massif have preserved high-grade structures. In the Zaza Zone, most of the sampled serpentinites only underwent low-grade metamorphism and the sample that underwent eclogitic conditions is strongly retrogressed. Low-grade serpentinites show pseudomorphic textures in thin section, a mixture of chrysotile, poorly crystallised serpentine and minor lizardite. High-grade samples, characterised by non-pseudomorphic textures, mainly consist of antigorite, associated to minor chrysotile. Transmission electron microscopy shows that antigorite from preserved samples (Escambray Massif) displays few microstructural defects such as stacking faults or modulation dislocations, in contrast to the higher density of defects encountered in highly retrogressed serpentinites (Zaza Zone). We thus propose that the record of high metamorphic grade in matrix antigorite is best characterised by the elimination of structural defects.

Key-words: Central Cuba, serpentine minerals, high pressure, HRTEM.

1. Introduction

Serpentinites, resulting from the hydration of ultramafic rocks, are frequently outcropping in convergent geodynamic settings. In non-accretionary subduction systems such as the Mariana arc, they are recognised in seamounts (e.g. Fryer & Fryer, 1987; Fryer *et al.*, 1999). These rocks are also commonly associated with high-pressure rocks in paleosubduction zones (*e.g.,* Belluso *et al.*, 1994, Hermann *et al*., 2000 and Schwartz *et al*., 2001, for the Alps; Guillot *et al.*, 2000, 2001; for the Himalaya; Millan & Somin, 1985, and Piotrowska, 1993, for Cuba). Recent studies have shown that serpentinites play a key role in recycling water in the mantle (Ulmer & Trommsdorff, 1995; Schmidt & Poli, 1998) and in the exhumation of the HP-LT rocks in subduction zones (Scambelluri *et al*, 1995; Guillot *et al.*, 2000, 2001; Schwartz *et al*., 2001). However, serpentinites are considered poor indicators because of the lack of reliable tools to estimate the metamorphic conditions they underwent and, thus, their P-T path along the subduction zones. This arises from the large stability field of serpentine minerals, which covers a large part of the subduction physical conditions (Fig. 1).

However, the transitions between the different serpentine varieties give some insights into the metamorphic conditions. Serpentine minerals, which are trioctahedral 1:1 phyllosilicates of ideal formula $Mg_3Si_2O_5(OH)_4$, display four main structural varieties. They are distinguished on the basis of their microstructures. Lizardite is characterised by a planar structure, chrysotile displays a cylindrical wrapping of the 1:1 layers, and antigorite has a modulated structure with inversion of the polarity of the layers (*e.g.,* Wicks & O'Hanley, 1988). A less well known variety is polygonal serpentine, which alternates flat and curved microstructures along the layers (*e.g*., Baronnet *et al.,* 1994). According to the phase diagram proposed by Berman *et al.* (1986), the appearance of the different serpentine varieties is mainly governed by temperature (Fig. 1). This is consistent with field evidence: in serpentinites from high-grade terranes, antigorite is the main matrix variety (*e.g*. Scambelluri *et al.*, 1995;

DOI: 10.1127/0935-1221/2002/0014-0905
0935-1221/02/0014-0905 $ 4.50

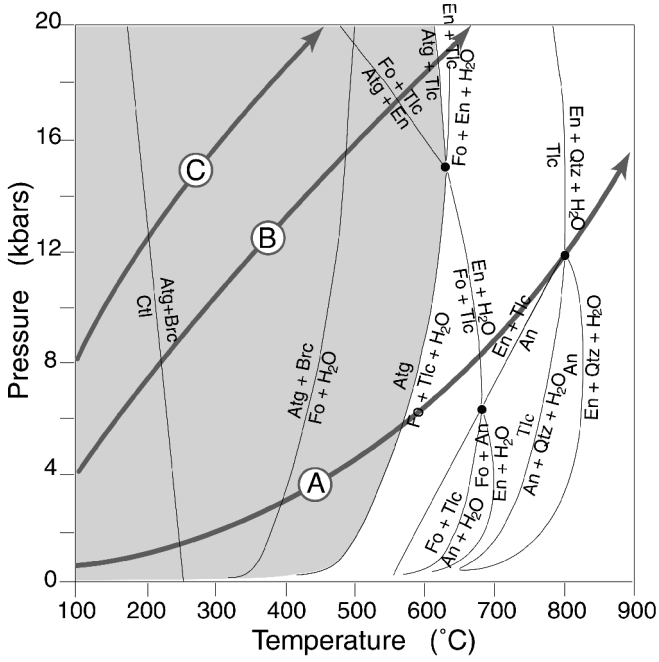

Fig. 1. P-T relationships between chrysotile (Ctl), antigorite (Atg), brucite (Brc), forsterite (Fo), talc (Tlc), enstatite (En), anthophyllite (An), quartz (Qtz), and H_2O in the MgO-SiO_2-H_2O system (after Berman *et al.*, 1986). The arrows correspond to three modelled slab geotherms representing the P-T conditions along the slab-mantle interface at 0 (A), 5 (B) and 10 (C) Ma after the initiation of the subduction (from Peacock, 1990).

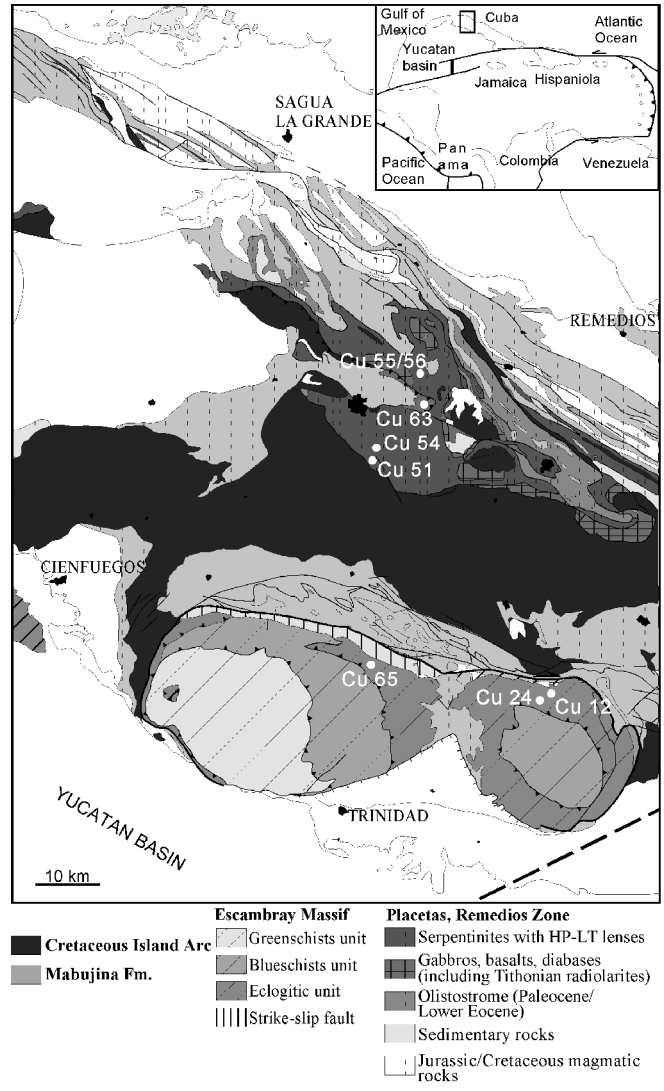

Fig. 2. a) General map of the Caribbean area; b) Geological map of the central part of Cuba (redrawn after Millan, 1993) and location of the samples.

Trommsdorff *et al.*, 1998; Guillot *et al.*, 2001). On the other hand, low-grade serpentinites, such as those found in oceanic lithosphere mainly consist of lizardite and chrysotile (Aumento, 1970; Aumento & Loubat, 1971; Prichard, 1979). However, recent works have underlined the importance of pressure (Wunder *et al.*, 1997, 2001; Ulmer & Trommsdorff, 1995) as well as chemistry (Caruso & Chernosky, 1979; Mellini, 1982) and departure from equilibrium (Grauby *et al.*, 1998) on the appearance of the different structural varieties. In subduction settings, characterised by high-pressure and low-temperature conditions (Fig. 1), antigorite is the most stable variety (Scambelluri *et al.*, 1995; Ulmer & Trommsdorff, 1995). The polysomatism of this variety was investigated by transmission electron microscopy (TEM) by Mellini *et al.* (1987) and Wunder *et al.* (2001), who showed a correlation between the *m*-value (*m* = number of tetrahedra in a single chain along the wavelength) and temperature.

The aim of this work was to tie the metamorphic conditions with the microstructures of serpentine minerals in samples from Central Cuba, a paleo-subuction zone. The metamorphic conditions undergone by the serpentinites, were established on the basis of field evidence and petrological study of the associated metabasites and serpentinites. We characterised the microstructures of serpentine minerals by TEM and selected-area electron diffraction (SAED), paying special attention to the amount of structural defects in antigorite crystals.

2. Geological setting and location of the samples

2.1. Geological setting

The margins of the Caribbean plate are characterised by the Lesser and Greater Antillean arcs, related to active and paleo-subduction zones, respectively. The Eocene to Recent Lesser Antillean arc stretches from the continental margin of South America (eastern Venezuela) up to the Anegada Passage (Fig. 2), on the eastern margin of the Caribbean plate. In this global convergent context, the island of Cuba appears as a series of accreted terranes of both continental and oceanic material, younger than Jurassic (Iturralde-Vinent, 1994).

Meyerhoff & Hatten (1968) divided Cuba into three major blocks: (1) Western Cuba, characterised by Jurassic sediments correlated with Jurassic continental beds in Central America and Jurassic sediments in the Gulf of Mexico; (2)

Central Cuba; and (3) Eastern Cuba, an uplifted part of the Cayman Rise.

Central Cuba is divided from NE to SW into four major tectonostratigraphic belts (Pardo, 1975). Zone 1 consists of dolomites, anhydrite-limestones, pelagic limestones and marls of Upper Jurassic to Tertiary age; and represents the southern edge of the Bahama-Florida Platform. Zone 2 consists of pelagic limestones, calcareous turbidites and radiolarian cherts of Tithonian to Maastrichtian age and represents the southward deep-water-facies extension of Zone 1. Zone 3 or Zaza Zone consists essentially of an allochthonous oceanic unit containing metabasites lenses embedded in a strongly deformed serpentinite matrix (Piotrowska, 1993). It represents an accretionary prism created during the southward subduction of the Atlantic plate and responsible for the development of the Upper Cretaceous arc. The Zaza Zone is tectonically juxtaposed by a sinistral strike-slip fault to the south against a thick sequence of Cretaceous volcanic-arc and sedimentary rocks intruded by granitoids and affected by recumbent folds to the south. This arc sequence thrusts towards the south over the Mabujina formation and the Escambray Massif (Zone 4). The Escambray massif is composed of carbonate and terrigenous metasediments, lenses of well-preserved serpentinites a few metres to several hundred metres in size, and metabasic rocks. The rocks, which are Jurassic to Cretaceous in age according to paleontological evidence, form two structural domes connected by a narrow bridge beneath a Paleogene cover (Millan & Somin, 1985). It is a metamorphic massif with nappe structures. From top to bottom of the nappe pile, three metamorphic units are distinguished (Millan & Somin, 1985): unit I shows greenschist facies metamorphic conditions; unit II is characterised by lawsonite-blueschist facies rocks; unit III has undergone zoisite-eclogitic conditions.

Due to the abundance of serpentinites and to their contrasted relationships with the metamorphic rocks, the Escambray massif and the Zaza Zone are well-suited areas for the study of serpentinites in a convergent settings.

2.2. Location of the samples

Samples of serpentinites and associated metabasites were collected in the Escambray Massif and in the Zaza Zone (Fig. 2). Special attention was paid to the structural relationships between the collected serpentinites and the associated metamorphic rocks. In the Escambray Massif, serpentinites form lenses associated to eclogitic metabasite lenses, and are embedded in a matrix of metasediments. In the Zaza Zone, serpentinites consist in a matrix which embeds metabasites lenses. On each associated metabasite, a petrological study was performed in order to evaluate the metamorphic conditions they underwent.

In the Escambray massif, the samples Cu12, Cu24, and Cu65 come from the serpentinite lenses in metamorphic unit III. The mineral paragenesis in the associated metabasites is almandine-rich garnet + omphacite (Jd_{40}) $\pm$ glaucophane + phengite (Si ~ 3.4 pfu) + paragonite + zoisite + quartz + rutile, without evidence of retrogression. This indicates eclogite metamorphic facies conditions characterised by minimal pressure conditions of 12 kbar and temperature above 450°C (*e.g.*, Spear, 1993).

In the Zaza Zone, Cu51, Cu54, Cu55, and Cu56 samples originate from the serpentinite matrix embedding the metabasites lenses. In the southern part of the zone, serpentinite Cu 54 was collected from the eclogite-embedding matrix. The metamorphic paragenesis in the metabasalts is defined by the eclogitic assemblage almandine-rich garnet + omphacite (Jd_{45}) + phengite (Si ~ 3.4 pfu) + paragonite + zoisite + quartz + rutile. The secondary paragenesis pyrope-rich garnet + magnesio-hornblende/pargasite + plagioclase + quartz + ilmenite is evidence for partial retrogression under high-pressure overprint. This paragenesis is reached in high amphibolite-facies conditions (over 3 kbar, at temperatures above 500°C, *e.g.*, Spear, 1993). Northwards, samples Cu 55 and Cu 56 are from a slightly serpentinized peridotite. Associated metabasic rocks are characterised by a low-pressure amphibolitic assemblage of hornblende + plagioclase + epidote + quartz + ilmenite without evidence of high-pressure minerals suggesting pressure conditions < 6 kbar and temperature of 400-500°C (*e.g.*, Spear, 1993). Cu 51 was sampled from the serpentinite matrix, rather close to Cu 54. However, this sample was collected in a shear zone and is closely associated with arc-related gabbro (magmatic clinopyroxene + plagioclase) that underwent only low-grade greenschist-facies recrystallisation (300-400°C and P < 6 kbar (*e.g.* Spear, 1993) characterised by an assemblage of chlorite ± albite ± actinolite ± quartz ± titanite. Similarly, sample Cu 63 comes from the arc sequence and is also associated with fresh greenish gabbros, suggesting that the associated serpentinite sample only underwent oceanic hydrothermal metamorphism.

3. High-resolution transmission electron microscopy

TEM imaging was performed with a JEOL 2000FX high-resolution transmission electron microscope at the CRMC^2-CNRS facility (Marseille, France). The operating conditions were: 200 kV accelerating voltage, a point-to-point resolution of 2.8 Å, and a side entry, double-tilt (± 30°) specimen holder. The TEM specimens were extracted from petrographic thin sections glued with Lakeside® thermofusible resin on a glass slide. Single-hole copper TEM grids were glued with araldite® on selected areas of the sections. Specimens were removed by drilling around the Cu grids and heating the resin. Prior to TEM observations, the specimen were thinned to perforation through ion-beam milling (GATAN 600 Duomill) and carbon-coated.

TEM allows an accurate determination of serpentine varieties. Conventional imaging reveals the texture and the occurrence of chrysotile, easily identified by its tubular microstructure. Polygonal serpentines would be conspicuous because of their larger diameters, and could be ascertained by orienting fibres along the tube axes. Antigorite is easily recognised by its modulated structure, giving rise on SAED patterns to superstructure spots in the $\mathbf{a}^*$ direction aside the normal reflections (*e.g.*, Spinnler, 1985). When observed in the [100] direction, *i.e.*, along the modulation direction, an

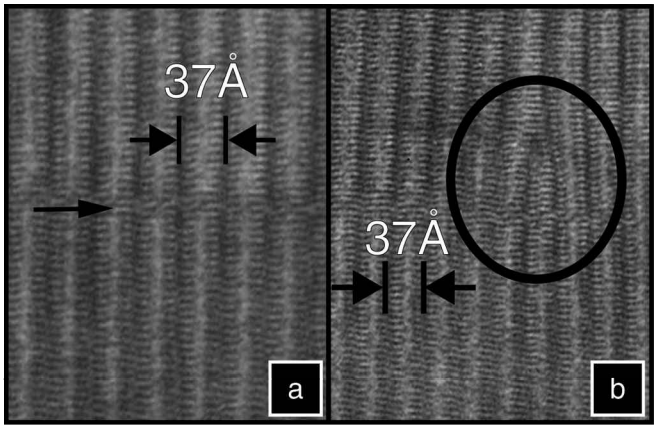

Fig. 3. Commonly occurring defects in antigorite microstructures. a) The arrow indicates a stacking defect. b) A modulation dislocation is circled.

tigorite can be misidentified for lizardite. The uncertainty can be resolved either by tilting the sample until the Ewald sphere cuts some superstructure spots, or by looking for cleavages. Cleavages are a very common feature in lizardite, but are never observed at the TEM scale in antigorite, due to the presence of Si-O-Si bonds along the **c*** direction.

As antigorite is the most common variety in completely serpentinized samples, we paid special attention to the possible variations of its microstructures. Variations of the modulation wavelength (*A*) have been observed by several authors (Kunze, 1961; Uehara & Kamata, 1994; Mellini *et al.*, 1987; Uehara, 1998; Wunder *et al.*, 2001). Defects in antigorite are complex (Spinnler, 1985), and include modulation dislocations and a variety of stacking sequences and faults (Fig. 3). To access these parameters, antigorite crystals were oriented along the [010] zone axis.

4. Petrography

4.1. Escambray serpentinites

The three samples Cu 12, Cu 24 and Cu 65, from the eclogitic unit of the Escambray massif, are entirely serpentinised and display non-pseudomorphic textures. The chemical analyses revealed serpentine compositions close to the Mg end-member, with however a few percent substitution of Mg and Si by Al and Fe, depending on sample (Table 1). Raman spectroscopic measurements, allowing a quick identification of the different serpentine varieties (Lemaire, 2000), revealed antigorite as the main variety. Serpentinite Cu 65, sampled in the western dome of the Escambray massif, is characterised by typical interpenetrative texture (Fig. 4a). Antigorite, which is the most recognisable serpentine variety, occurs in the matrix as blades, with size varying between a few tens of micrometres to several millimetres. Serpentinites Cu 12 and Cu 24, sampled in the eastern dome of the massif, display a foliation defined by the preferred orientation of the antigorite blades and elongated oxides (Fig. 4b).

This same foliation was recognised in the metabasite associated to Cu 24. A few blades cut this foliation, suggesting

Table 1. Representative electron microprobe analyses of serpentine minerals from Cubean samples (Cameca SX 100, Clermont-Ferrand, 15 kV, 10 nA). (atg: antigorite, chrs: chrysotile)

Samples	Cu12	Cu12	Cu24	Cu24	Cu65	Cu54	Cu51	Cu63
	atg	atg	atg	atg	atg	atg	chrs	chrs
SiO_2	41.65	41.55	42.39	41.05	41.09	42.65	42.78	41.93
Al_2O_3	3.45	3.14	2.77	2.65	2.93	1.42	0.31	0.77
FeO	4.15	3.65	4.28	4.02	8.30	7.56	4.06	5.20
MgO	37.37	37.53	37.28	37.40	33.66	35.02	36.72	37.87
total	86.62	85.86	86.73	86.13	85.98	86.65	86.81	85.77
				Atoms per formula unit				
Si	1.96	1.97	1.99	1.99	1.99	2.04	2.06	2.01
Al	0.19	0.17	0.15	0.15	0.17	0.08	0.01	0.04
Fe	0.16	0.14	0.17	0.16	0.34	0.30	0.17	0.21
Mg	2.62	2.65	2.61	2.64	2.43	2.49	2.68	2.70
total	4.94	4.94	4.92	4.94	4.93	4.92	4.93	4.97

Structural formulae are calculated on the basis of 7 equivalent oxygens.

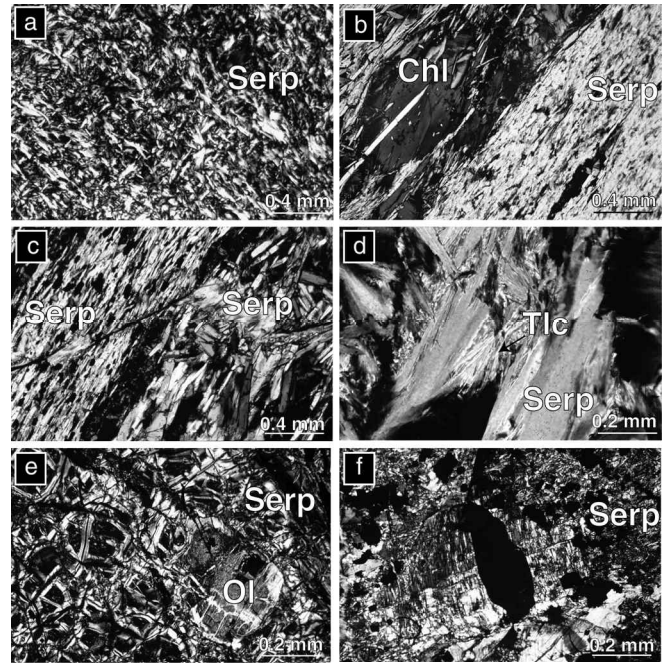

Fig. 4. Serpentinite textures: microphotographs, crossed nichols. a) Non-pseudomorphic texture in serpentinite Cu 65. b) Serpentinite Cu 12 displaying serpentine blades and a vein filled with chlorite oriented in the same direction. c) Late serpentine vein cutting the preferred orientation in serpentinite Cu 12. d) Serpentine blades associated to talc in serpentinite Cu 54. e) Pseudomorphic texture (mesh rims with olivine core) in serpentinite Cu63. f) Bastite texture in Cu 56.

limited retrograde recrystallisation. All samples contain oxides, which mostly consist of newly formed magnetite and, to a lesser extent, of relict chromian spinel inherited from the protolith. A few veins cut the foliation, indicating late deformation. In Cu 12 and Cu 65, a few cross-fibres veins consisting of flexuous serpentines, identified as a mixing of chrysotile and lizardite by Raman spectroscopy, presum-

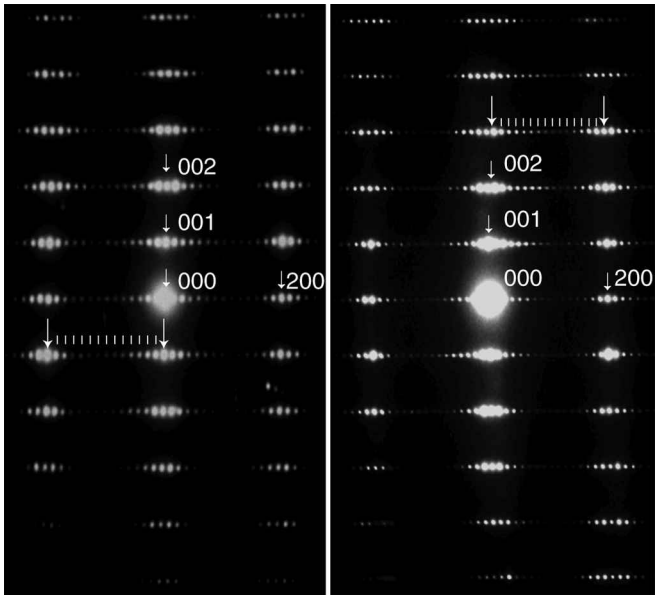

Fig. 5. Representative SAED patterns of ordered antigorite crystals from Cu 65 recorded along the [010] zone axis. a) The modulation display 13 superstructure spots between two substructure spots indicated by the white arrows. b) The modulation displays 14 superstructure spots. The patterns are indexed according to the subcell of serpentine minerals.

ably developed during late fluid circulations (Fig. 4c). Cu 24 also locally reveals a concentration of opal (identified by TEM) embedding small diopside grains in individualised beds concordant with the foliation, probably arising from localised fluids circulation.

4.2. Zaza Zone serpentinites

Five samples were collected in this zone (Cu 51, Cu 54, Cu 55, Cu56, and Cu 63). We did not observe any preferred orientation of the minerals in these rocks, suggesting that they did not undergo or preserve any ductile deformation. Sample Cu 54, associated to the eclogite-facies metabasite displays a non-pseudomorphic texture, similar to that observed in serpentinite Cu 65 from the Escambray Massif. The Raman spectroscopic investigation of the former sample indicates that antigorite is the most common serpentine variety. Sample Cu 54 is also characterised by the occurrence of talc, which seems to develop at the expense of antigorite (Fig. 4d). Cu 55 and Cu 56 correspond to more or less serpentinised peridotites associated to the low-pressure amphibolite facies metabasite. Cu 55 displays a lower rate of serpentinisation than Cu 56. In these rocks, relict olivine and pyroxene often remain but serpentine veins, recognised as chrysotile mixed with minor lizardite by Raman spectroscopy, devel-

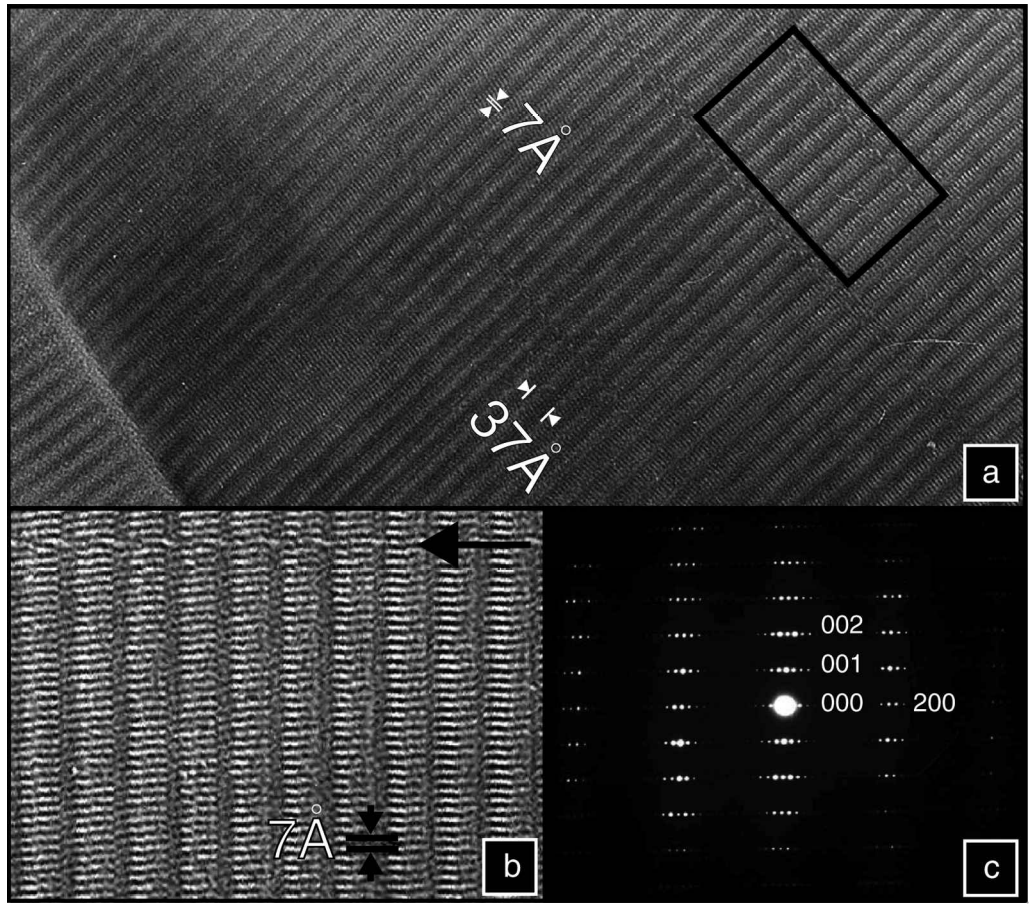

Fig. 6. a) High-resolution lattice image of ordered serpentine in Cu 65 sample seen along [010] zone axis; b) magnification of the framed zone; c) a corresponding SAED pattern.

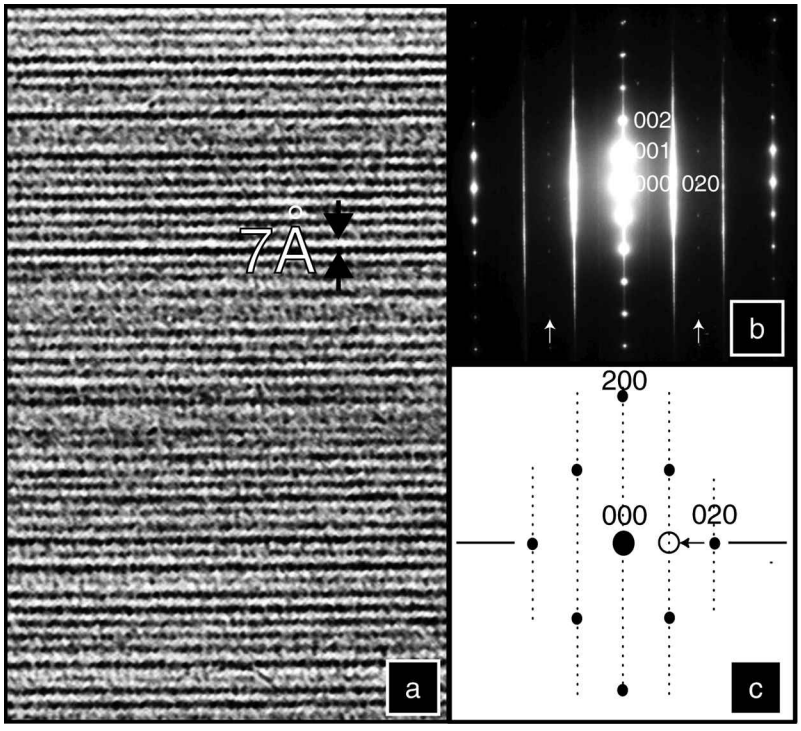

Fig. 7. a) High-resolution lattice image of antigorite in Cu 65 seen along the [100] zone axis. b) Associated SAED pattern. The white arrows indicate the 03*l* spots due to the modulated structure. c) Reciprocal space seen in the [001] direction. The horizontal line corresponds to the trace of Ewald sphere for [100] patterns. The pattern is indexed according to the C-centred subcell of serpentine. The circle outlines the position of the 0*kl* (*l* odd) spots due the superstructure on the trace of the Ewald sphere for [100] patterns (horizontal line).

oped in the cleavages of pyroxene and fractures of olivine. The minerals that are entirely serpentinised in these samples display pseudomorphic textures. Samples Cu 51 and Cu 63, from the arc sequence, are entirely serpentinised and display pseudomorphic (mesh and bastite) textures (Fig. 4e and f). According to the Raman spectra, these samples mostly consist of a mixing of chrysotile and lizardite.

5. Results of HRTEM imaging and SAED

5.1. Escambray serpentinites

The SAED patterns obtained on samples Cu 12, Cu 24, and Cu 65 confirm that the most commonly occurring mineral in the matrix is antigorite (Fig. 5, 6). Superstructure spots defining the supercell surround the *h*0*l* spots of serpentine minerals (substructure). On the representative SAED patterns of Fig. 5, there is a rational division by superstructure spots of the reciprocal distance between two substructure spots, implying that the modulation is commensurate with the substructure. Thirteen satellites can be counted between substructure spots on Fig. 5a, and fourteen in Fig. 5b. The wavelength of antigorite modulations can be obtained by the formula $A = (n + 1)\, a/2$, where n is the number of satellites, and a is the 5.3 Å lattice parameter common to layer silicates. Thus, these antigorites have a modulation wavelength of 37 Å and 40 Å, respectively. It must be noted that the most commonly occurring wavelength in Cubean samples is 37 Å. These values agree with those obtained by Zussman *et al.* (1957). These SAED patterns also indicate that antigorites are perfectly ordered in this direction of observation. Indeed, no streaking between superstructure spots is visible along the $\mathbf{c}^*$ direction, indicating a perfect 1-layer stacking sequence. The fact that the superstructure spots do not show diffuse streaking along $\mathbf{a}^*$ indicates the regularity of the modulation wavelength over the selected area (about 3 μm^2). Finally, the superstructure spots line up perfectly toward the substructure reflections along $\mathbf{a}^*$, indicating the absence of offset in the stacking of these antigorites (Spinnler, 1985). The *A* parameter can also be measured on HRTEM images (Fig. 6), although less precisely than on SAED patterns. Fig. 6 shows an antigorite crystal with a modulation of 37 Å, in agreement with the values obtained from SAED. The imaging confirms the structural perfection observed on SAED patterns, with a highly regular modulation wavelength, and rare stacking faults.

However, stacking disorder along the $\mathbf{c}^*$ axis was commonly observed in the antigorites of the Escambray when viewed along [100]. SAED along the [100] observation direction (Fig. 7) shows intense streaking on the 0k*l* lateral rows, $k \neq 3n$. This indicates extensive stacking disorder of the layers, each layer being randomly shifted by 0, +1/3 **b** or -1/3 **b** relative to the previous one. The disorder is confirmed by high-resolution imaging (Fig. 7a). When observed along the [100] direction, neither SAED patterns nor high-resolution images display modulations. However, faint spots are often visible at the place of 0*kl* (*k* odd) forbidden reflections. These spots do not indicate a superstructure along **b**, but are the trace of the superstructure reflections of antigorite cutting the Ewald sphere (Fig. 7c). Antigorites in the same sample appear to be perfectly ordered when observed along [010].

Escambray samples also display some late veins, essentially consisting of chrysotile fibres. Veins can develop inside the crystals of antigorite, but no genetic relationship has been noticed between the two species in these samples.

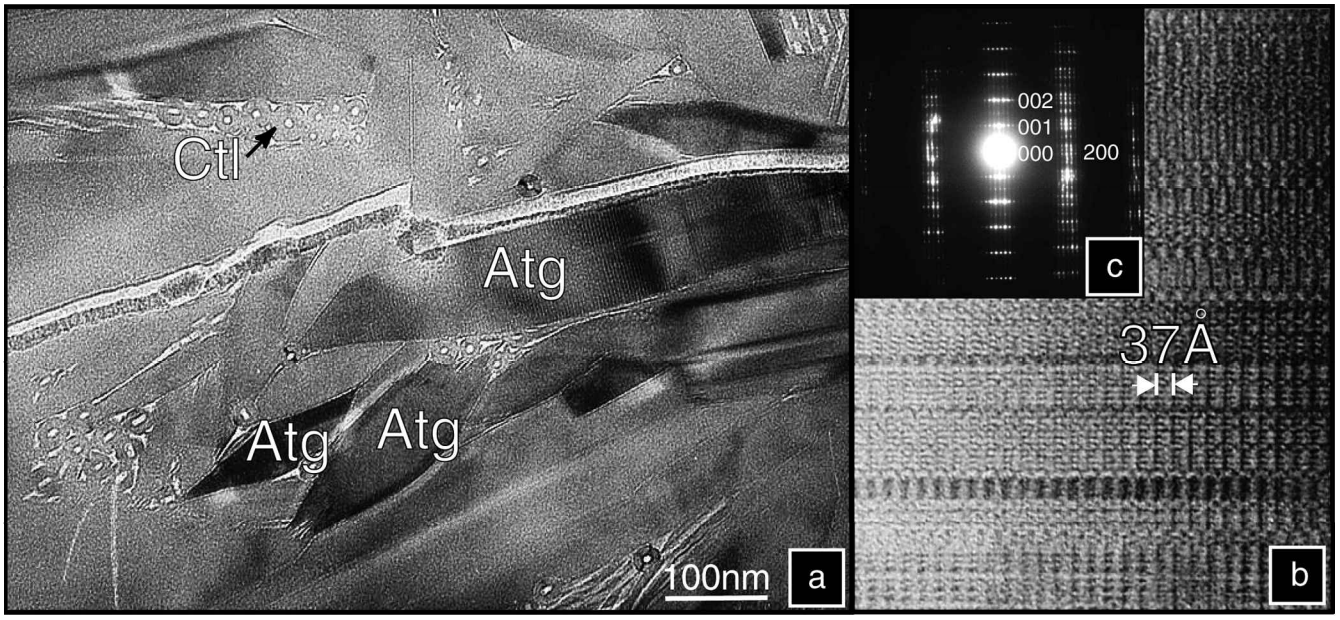

Fig. 8. a) Low magnification TEM image of vein antigorites associated to chrysotile in Cu 54 sample (Zaza zone). b) High-resolution lattice image of disordered antigorite. c) Associated SAED pattern.

5.2. Zaza Zone serpentinites

Sample Cu 54, associated to the eclogitic metabasite, contains antigorite. A few matrix antigorites are ordered, but on average they display a higher abundance of defects than antigorites from the Escambray Massif. The most common defects consist of stacking faults and modulation dislocations (Fig. 4, 8) which can lead to highly disordered structures. Low magnification images show almond-shaped matrix antigorites. Viti & Mellini (1996) have described this morphology at a higher scale in vein antigorites (Fig. 8a). The SAED patterns along the [010] zone axis show diffuse streaks binding the diffraction spots in the $\mathbf{c}^*$ direction, confirming the large amount of stacking disorder (Fig. 8c). Reinforcements of the intensity halfway along the streaks suggest a tendency to a 2-layer stacking sequence, which shows up in high-resolution images as intergrown slabs of 1-layer and 2-layer periodicity along $\mathbf{c}^*$ (Fig. 8b). The modulation wavelength is, as in antigorite from Escambray samples, constant around 37 Å. Antigorites from Cu 54 are frequently associated to chrysotile, and there is a genetic relation between those species: chrysotile seems to develop at the expense of antigorite crystals (Fig. 9).

Sample Cu 51, from the arc sequence, does not reveal antigorite but chrysotile as the major constituent. In Cu 63 serpentinite, chrysotile, associated with poorly crystallised serpentine, is the most abundant serpentine mineral. Locally, textural relationships between those two varieties can be observed. The poorly crystallised serpentine seems to act as a precursor for the crystallisation of chrysotile fibres. Cu 55 and Cu 56 are characterised by major chrysotile in the cleavages and fractures of the primary minerals. In Cu 56, minor lizardite, associated to chrysotile, is observed. Antigorite was not observed in those samples.

6. Discussion

6.1. Metamorphic conditions

One of the fundamental problems related to the study of serpentinites is the evaluation of the metamorphic conditions they underwent. This is especially critical in a subduction setting, because antigorite is stable over a large part of the P-T field reached during burial and exhumation (Fig. 1). In the absence of associated minerals such as olivine or enstatite, there is no reliable geothermometer nor geobarometer which can be applied to these rocks. Thus, the field relations and sample selection becomes critical.

In the Escambray massif, the collected serpentinites and eclogites are associated within the same lenses, embedded in a matrix of metasediments. Moreover, serpentinite Cu 24 displays the same preferred planar orientation as the foliated eclogite. These observations suggest that serpentinites and associated eclogites shared the same metamorphic history, as in the Catalina schist terrane (Bebout & Barton, 1989). The mechanical weakness of the surrounding matrix of metasediments and the absence of retrogression in the eclogitic metabasites suggest that the associated serpentinites lenses escaped retrogression as well. Thus, we propose that the Escambray serpentinites have recorded and preserved eclogite-facies conditions.

In the Zaza zone, serpentinites are embedding the metabasites as observed in the Voltri eclogitic massif (Scambelluri *et al.*, 1995; Hermann *et al.*, 2000) or the Monviso eclogitic massif in the Alps (Schwartz *et al.*, 2001). These studies and the work of Guillot *et al.* (2001) in the Himalaya suggest that serpentinites, due to their low density (2.75 g/cm^3) and low viscosity (< 10^{20} Pa.s) act as a lubricant in subduction zone and provide a mechanism of exhumation for the

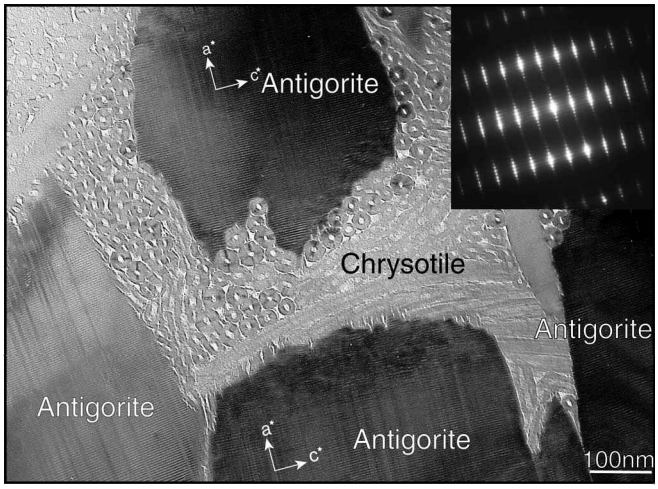

Fig. 9. Low magnification TEM image of a single crystal of antigorite retrogressed into chrysotile fibers in Cu 54 sample (Zaza Zone) and corresponding SAED pattern.

eclogitic rocks. These studies also clearly show that serpentinites and the associated metabasites have shared similar metamorphic history. The serpentinites from the Zaza Zone are embedding the lenses of eclogites. Consequently they must be more severely affected by the late retrogressive metamorphic evolution. As the serpentinite Cu 54 is associated to eclogites that are partly overprinted under high-pressure amphibolitic conditions, it must have strongly recrystallised during the warming up and, thus, probably largely records this part of the metamorphic history.

Samples Cu 55 and Cu 56 also probably record metamorphic conditions similar to those undergone by the associated low-pressure amphibolites. Indeed, the preservation of the pseudomorphic texture and of a large amount of primary minerals implies the absence of important burial. Finally, Cu 51 and Cu 63, associated to the arc sequence, underwent only a low-grade hydrothermal alteration.

6.2. Relationship between serpentine microstructures and metamorphic conditions

The samples that have undergone eclogitic conditions (Cu 12, Cu 24 and Cu 65 from the Escambray Massif, and Cu 54 from the Zaza zone) show non-pseudomorphic textures and display antigorite as the major matrix constituent. In low-grade samples (Cu 51, Cu 55, Cu 56, Cu 63 from the Zaza Zone), we observed pseudomorphic textures formed by a mixing of chrysotile, minor lizardite, and poorly crystallised serpentine. The phase diagram (Fig. 1) would predict the occurrence of antigorite in the amphibolitic serpentinite (Evans *et al.*, 1976; Berman *et al.*, 1986). Instead, the samples Cu 55 and Cu 56 only display chrysotile and minor lizardite. The absence of antigorite could be explained by an important amount of aluminium in the serpentine mineral. Indeed, according to Caruso & Chernosky (1979), the occurrence of aluminium in lizardite tends to increase its stability field in the MASH system (MgO-Al_2O_3-SiO_2-H_2O). Actually, for a composition of $Mg_{5.5}Al_{0.5}Si_{3.5}Al_{0.5}O_{10}(OH)_8$ (around 9% wt Al_2O_3), its thermal stability is higher than that of antigorite under low-pressure conditions. This promotion of the formation of flat-layer structure with increasing temperature was also shown by Mellini (1982) on significantly substituted lizardite-1*T*. Grauby *et al.* (1998) observed under low-pressure conditions that the addition of aluminium in serpentines synthesised from gels tend to stabilise the planar variety lizardite. However, microprobe analysis of serpentinites from the Zaza Zone revealed less than 1 wt% of alumina in serpentine (Table 1). This amount of Al is insufficient to explain the absence of antigorite in the amphibolitic serpentinite. Moreover, aluminium tends to stabilize lizardite, whereas the sample in question mostly consists of chrysotile, the cylindrical variety. Thus, as we only observe antigorite in the high-grade samples, we propose that pressure can play a role in the appearance of the structural varieties of serpentine minerals in the matrix, even if this factor does not appear to be discriminant in the P-T stability-field diagram of Berman *et al.* (1986). This is in agreement with recent experimental work by Wunder *et al.* (1997, 2001), who was successful in the synthesis of purely magnesian antigorite from stoichiometric mixtures only at pressures above 1 GPa. Iishi & Saito (1973) synthetised antigorite under conditions around 1.8 kbar and 500°C, but they started from non-stoichiometric mixtures. To our knowledge, no other successful synthesis of antigorite under low-pressure conditions is reported, despite several attempts.

Among the eclogitic serpentinites, we have distinguished preserved and retrogressed serpentinites on the basis of field relations and the petrological study. Escambray serpentinites, preserved from retrogression by the embedding metasediments, display antigorite as the main matrix mineral. They occur as blades and TEM study reveals only few defects affecting their microstructures. Chrysotile is also locally observed, but in small amount, and essentially within microveins. On the other hand, Zaza Zone eclogitic serpentinite, affected by a warming up during overprint, is characterised by antigorites which display a large number of defects, such as stacking faults or modulation dislocations. Moreover, their almond-shaped morphology differs from the Escambray antigorite shapes. This morphology has already been observed macroscopically by Viti & Mellini (1996) in veins from Elba Island. Thus, clearly, antigorite can record variations in its microstructures in relation with the metamorphic conditions. We propose that highly ordered antigorite (small amount of structural faults) is a feature of high-grade serpentinites whereas disordered antigorite (high amount of structural faults) characterises lower-grade metamorphic conditions. It must be noted that this ordering of antigorite with pressure is a tendency, established on the basis of numerous observations from TEM after orienting crystals from various samples. So far, we lack a method that would allow quantitative estimation of disorder in antigorite at a macroscopic scale. Our attempts with X-ray diffraction failed, due to preferential orientation problems and mixture with other phases such as chrysotile.

Correlating the variations of antigorite microstructures to the metamorphic conditions has already been tested. Mellini *et al.* (1987) and Wunder *et al.* (2001) showed a decrease of

the modulation wavelength with temperature. Uehara & Kamata (1994) described antigorite with a large supercell formed under low-temperature and high-pressure (pumpellyite-actinolite facies) conditions. They also showed the important role of the chemical composition (substitution rate) onto the modulation wavelength. This implies that modulation wavelength is not only T-dependent, but also chemistry-dependent, leading to an ambiguous determination of the metamorphic grade as a function of the modulation wavelength. Moreover, Viti & Mellini (1996) reported variability of antigorite superperiodicity without any relation to metamorphic grade in vein antigorites. Thus, according to these statements and as we did not observe clear variation of the modulation wavelength, we propose here that the record of the metamorphic grade in matrix antigorite could better be dicussed in terms of amount of defects in the microstructures instead of modulation wavelength variability.

The effect of pressure on ordering in phyllosilicates has been investigated by Jullien *et al.* (1996). These authors showed that cookeite is perfectly ordered under blueschist-facies conditions whereas it is disordered under lower pressure conditions. Similar results were found in talc and ferromagnesian chlorites (Jullien, 1995). The author suggests that the compression of the structure is accompanied by an ordering of the microstructures, producing ordered sequences, which would be more compact, and thus more stable.

7. Conclusion

In Central Cuba, different metamorphic units, ranging from eclogitic to low-grade metamorphic conditions, characterise this paleo-subduction zone context. Antigorite occurs as a matrix phase only in high-grade serpentinites, but was not formed in an amphibolitic sample. The amount of aluminium in this sample being insufficient to explain the lack of antigorite, we suggest that pressure can play a role in the occurrence of serpentine structural varieties. In high-grade serpentinites, TEM revealed that antigorite, the main variety, displays few structural defects only when in preserved eclogitic samples, whereas it shows a large amount of faults in retrogressed samples. Moreover, we found no clear variability of the modulation wavelength with metamorphic grade in Cubean samples. Thus, we propose that the record of increasing metamorphic grade in matrix antigorite could be better characterised by the elimination of structural defects. A more systematic characterisation of natural serpentinites is necessary to validate this tendency. Moreover, other factors such as fluid-rock ratio, kinetics of reaction, deformation and crystal growth mechanisms could also influence the occurrence of serpentine minerals and have to be investigated.

Acknowledgements: The authors are grateful to C. Chopin, M. Mellini and to B. Wunder who largely contributed to improve the original manuscript. Special thanks go to M. Clermont for the quality of the thin sections and to S. Nitsche for the technical assistance with TEM. This work benefited from the support of the "Institut National des Sciences de l'Univers" to the "Center for in situ vibrational spectroscopy" and to the CRMC^2 TEM National Facility, as well as for the "Action Thématique Innovante" programme (CNRS).

References

Aumento, F. (1970): Serpentine mineralogy of ultrabasic intrusion in Canada and on the Mid-Atlantic Ridge. *Geol. Surv. Canada Pap.*, 69-53.

Aumento, F. & Loubat, H. (1971): The Mid-Atlantic Ridge near 45° N; XVI. Serpentinized ultramafic intrusions. *Can. J. Earth Sci.*, **8**, 631-663.

Baronnet, A., Mellini, M., Devouard, B. (1994): Sectors in polygonal serpentine. A model based on dislocations. *Phys. Chem. Minerals*, **21**, 330-343.

Bebout, G. E. & Barton, M. D. (1989): Fluid flow and metsomatism in a subduction zone hydrothermal system: Catalina Schist terrane, California. *Geology*, **17**, 976-980.

Belluso, E., Compagnoni, R., Ferraris, G. (1994): Occurrence of asbestiform minerals in the serpentinites of the piemonte zone, Western Alps. *in* Giornata di studio in ricordo del Prof. Stefano Zucchetti, 57-66.

Berman, R.G., Engi, M., Greenwood, H.J., Brown, T.H. (1986): Derivation of internally-consistent thermodynamic data by the technique of mathematical programming: A review with application to the system MgO-SiO_2-H_2O. *J. Petrol.*, **27**, 1331-1364.

Caruso, L. & Chernosky, J.V., Jr (1979): The stability of lizardite. *Can. Mineral.*, **17**, 757-769.

Evans, B.W., Johannes, W., Otterdoom, H., Trommsdorff, V. (1976): Stability of chrysotile and antigorite in the serpentine multisystem. *Schweiz. Mineral. Petrogr. Mitt.*, **56**, 79-93.

Fryer, P. & Fryer, G.J. (1987): Origin of non-volcanic seamounts in a forearc environment. *in* "Seamounts. Islands and atolls". Keating, B., Fryer, P., Batiza, R. (eds.). Geophysical Monograph, American Geophysical Union, **43**, 61-69.

Fryer, P., Wheat, C.G., Mottl, M.J. (1999): Mariana blueschist mud volcanism: Implications for conditions within the sunduction zone. *Geology*, **27**, 103-106.

Grauby, O., Baronnet, A., Devouard, B., Soumacker, K., Demirjian, L. (1998): The chrysotile-polygonal serpentine-lizardite suite synthesized from a 3MgO-2SiO_2-excess H_2O gel. EMPG VII, Orléans, *Terra Nova suppl.*, **10(1)**, 24.

Guillot, S., Hattori, K.H., de Sigoyer, J. (2000): Mantle wedge serpentinization and exhumation of eclogites: Insights from Eastern Ladakh, Northwest Himalaya. *Geology*, **28**, 199-202.

Guillot, S., Hattori, K., de Sigoyer, J., Nägler, T., Auzende, A. L. (2001): Evidence of hydration of the mantle wedge and its role in the exhumation of eclogites. *Earth Planet. Sci. Lett.*, **193**, 115-127.

Hermann, J., Müntener, O., Scambelluri, M. (2000): The importance of serpentine mylonites for subduction and exhumation of oceanic crust. *Tectonophysics*, **327**, 225-238.

Ishii, K. & Saito, M. (1973) : Synthesis of antigorite. *Am. Mineral.*, **58**, 915-919.

Iturralde-Vinent, M.A. (1994): Circum-carribean tectonic and igneous activity and the evolution of carribean plate: Discussion. *Geol. Soc. Am. Bull.*, **85**, 1961-1962.

Jullien, M. (1995): Polytypisme, ordre d'empilement et interstratification dans la cookeite et les phyllosilicates non micacés du métamorphisme. Influence de la pression. Thesis report, Univ. Rennes, France, 226.

Jullien, M. , Baronnet, A., Goffe, B. (1996): Ordering of the stacking

sequence in cookeite with increasing pressure: An HRTEM study. *Am. Mineral.*, **81**, 67-78.

Kunze, G. (1961): Antigorit Strukturtheoretische Grundlagen und ihre praktische Bedeutung fur die weitere Serpentin-Forschung. *Fortschr. Mineral.* **39**, 206-324.

Lemaire, C. (2000): Application des spectroscopies vibrationnelles à la détection d'amiante dans les matériaux et à l'étude des serpentines. Thesis report. Univ. Paris VII, France, 152.

Mellini, M. (1982): The crystal structure of lizardite-1*T*: hydrogen bonds and polytypism. *Am. Mineral.*, **67**, 587-598.

Mellini, M., Trommsdorff, V., Compagnoni, R. (1987): Antigorite polysomatism: Behaviour during progressive metamorphism. *Contrib. Mineral. Petrol.*, **97**, 147-155.

Meyerhoff, A.M. & Hatten, C.W. (1968): Diapiric structures in Central Cuba. *Mem. Am. Assoc. Petrol. Geol.*, **8**, 315-357.

Millan, G. (1993): Evolucion de la estructura del macizo de Escambray, sur de Cuba central. Evolution of the structure of the Escambray Massif, south-central Cuba. *Ciencias de la Tierra y del Espacio*, **21-22**, 26-45.

Millan, G. & Somin, M.L. (1985): Nuevos aspectos sobre la estratigrafia del macizo metamorfico del Escambray. New aspects about the stratigraphy of the Escambray metamorphic massif. *Reporte de Investigacion del Instituto de Geologia y Paleontologia*, **2**, 74.

Pardo, G. (1975): Geology of Cuba. *in* "The gulf of Mexico and the Caribbean". Nairn, A.E.M. & Stehli, F.G. (eds.), 552-615.

Peacock, S.M. (1990): Fluid processes in subduction zone. *Science*, **248**, 329-337.

Piotrowska, K. (1993): Interrelationship of the terranes in Western and Central Cuba. *Tectonophysics*, **220**, 273-282.

Prichard, H.M. (1979): A petrographic study of the process of serpentinisation in ophiolites and the oceanic crust. *Contrib. Mineral. Petrol.*, **63**, 231-241.

Scambelluri, M., Müntener, O., Hermann, J., Piccardo, G.B., Trommsdorff, V. (1995): Subduction of water in the mantle: History of an Alpine peridotite. *Geology*, **23**, 459-462.

Schmidt, M.W. & Poli, S. (1998): Experimentally based water budgets for dehydrating slabs and consequences for arc magma generation. *Earth Planet. Sci. Lett.*, **163**, 361-379.

Schwartz, S., Allemand, P., Guillot, S. (2001): Numerical model of effect of serpentinites on the exhumation of eclogitic rocks: insights from the Monviso ophiolitic massif (Western Alps). *Tectonophysics*, **342**, 193-206.

Spear, F.S. (1993): Metamorphic Phase Equilibria and Pressure-Temperature-Time Paths. *Mineral. Soc. Am., Mon. Ser.*, 799.

Spinnler, G.E. (1985): HRTEM study of antigorite, pyroxene, serpentine reactions and chlorite. Ph.D thesis, Arizona State Univ., Tempe, Arizona.

Trommsdorff, V., Lopez Sanchez-Vizcaino, V., Gomez-Pugnaire, M.T., Muntener, O. (1998): High pressure breakdown of antigorite to spinifex-textured olivine and orthopyroxene, SE Spain. *Contrib. Mineral. Petrol.*, **132**, 139-148.

Uehara, S. (1998): TEM and XRD studies of antigorite superstructure. *Can. Mineral.*, **36**, 1595-1605.

Uehara, S. & Kamata, K. (1994): Antigorite with large supercell from Saganoseki, Oita Prefecture, Japan. *Can. Mineral.*, **32**, 93-103.

Ulmer, P. & Trommsdorff, V. (1995): Serpentine stability to mantle depths and subduction-related magmatism. *Science*, **268**, 858-861.

Viti, C. & Mellini, M. (1996): Vein antigorites from Elba Island, Italy. *Eur. J. Mineral.*, **8**, 423-434.

Wicks, F.J. & O'Hanley, D. (1988): Serpentine Minerals: Structure and petrology. *Reviews in Mineralogy*, Bailey, S.W. (ed.), 91-167.

Wunder, B., Baronnet, A., Schreyer, W. (1997): Ab-initio synthesis and TEM confirmation of antigorite in the system MgO-SiO_2-H_2O. *Am. Mineral.*, **82**, 760-764.

Wunder, B., Wirth, R., Gottschalk, M. (2001): Antigorite: Pressure and temperature dependence of polysomatism and water content. *Eur. J. Mineral.*, **13**, 485-495.

Zussman, J., Brindley, G.W., Comer, J.J. (1957): Electron diffraction studies of serpentine minerals. *Am. Mineral.*, **42**, 133-153.

Received 5 December 2000
Modified version received 1 February 2002
Accepted 21 March 2002